A nucleation – elongation mechanism for the self-assembly of side polar sheets of smooth muscle myosin

R.A.Cross, M.A.Geeves[1] and J.Kendrick-Jones

MRC Laboratory of Molecular Biology, Hills Road, Cambridge CB2 2QH and [1]Department of Biochemistry, University of Bristol School Of Medical Sciences, Bristol BS8 1TD, UK

Communicated by R.A.Crowther

Self-assembled filaments of smooth muscle myosin were observed by low dose electron microscopy to be flat side-polar sheets, in which the component molecules appeared straight and close-packed. Fraying experiments released small oligomers, in which molecules were staggered in parallel by about ±14 nm relative to two immediate neighbours, and were bound also to an antiparallel partner via a ~14 nm overlap at the very tip of the tail. We suggest a filament model which preserves these packing relationships. Adding stoichiometric amounts of MgATP to the filaments caused them to disassemble completely by progressive loss of material from their ends, at a limiting rate equivalent to about 2 monomers per second per end in physiological saline. The rate of the competing association reaction varied linearly with the monomer concentration, as determined in pressure-jump experiments. This suggests that myosin monomers, rather than dimers or higher oligomers, are the building blocks of these filaments. Shearing and annealing of assembled filaments appeared negligible on a time scale of a few hours. In consequence, filament number and filament length were dependent on the rate at which monomers were supplied to the assembly reaction, and on the number of filaments already present at the start of the assembly reaction.
Key words: 6S – 10S/coiled coil/myosin filaments/myosin self-assembly/side-polar/smooth muscle myosin

Introduction

All type II myosins self-assemble spontaneously at physiological ionic strength, and all are soluble, substantially as 6S monomers, at high ionic strength. If a step-reduction of ionic strength is imposed, then the assembly reactions are typically complete within a few seconds. To some extent the speed of this reaction has posed technical problems for the elucidation of its component steps, so that most previous studies have concentrated their attention on examining the steady state filament population, and on the free monomer population in equilibrium with it. The size-distribution of the assembled filament population, and the concentration of monomers in equilibrium with it, have been shown to be dependent on the ionic composition of the assembly buffer, on the rate at which the ionic concentrations in the solution approach their final value, and on the myosin concentration. On the other hand, the concentration of monomers in equilibrium with filaments is not dependent on the route by which the final conditions are obtained, but only on the final

conditions, and not at all on the myosin concentration, provided it is greater than a critical value (Josephs and Harrington, 1966,1968; Megerman and Lowey, 1981; Pollard, 1982; Kendrick-Jones and Citi, 1987).

Some kinetic studies have nonetheless been made. For striated muscle myosin filaments, Davis (1981, 1982, 1985; reviewed in Davis, 1988) has used pressure-jumps to perturb the assembly equilibria, and has measured rate and equilibrium constants for the in vitro self-assembly of skeletal muscle myosin at pH 8. He has argued on the basis of this data for an assembly mechanism involving the strictly sequential addition of parallel dimers to the filament ends. Much less is known about the kinetics of nonsarcomeric myosin self-assembly, yet these are the simpler, possibly ancestral, case. Sinard et al. (1989) recently found evidence for stepwise dimer – tetramer – octamer formation in Acanthamoeba myosin filaments formed by a downwards jump of ionic strength. Myosin filaments in these and other motile single cells assemble and disassemble dynamically and in a coordinated way, in order to produce force at particular stages of the cell cycle or in response to a chemotactic signal (Yumura and Fukui, 1985; Nachmias et al., 1989). In several of these systems force generation and filament assembly are both Ca-regulated, and to this extent at least, are coupled (Korn and Hammer, 1988; Citi and Kendrick-Jones, 1988; Spudich, 1990).

Smooth muscle myosin exhibits similarly dynamic self-assembly properties, and offers unique advantages as a model system for kinetic studies of myosin assembly. Its molecules equilibrate between two global conformations, the linear 6S form and the looped 10S form. In the looped conformation the myosin tail bends back on itself and appears to bind to the heads. This binding effectively locks the molecule into an inert conformation, unable either to self-assemble or to hydrolyse MgATP (or bind to actin; Cross, 1988). The release of molecules from this inert conformation is rate-limiting on assembly under most conditions (Cross, 1986). This, the first step on the assembly pathway, can be switched in kinetic experiments in vitro. It is possible that the same step is regulated in vivo.

Little is known about subsequent steps on the assembly pathway. Steady state studies have identified a large number of stable modes of self-interaction of myosin molecules, and the self-assembly pathway of smooth muscle myosin filaments could incorporate any or all of these. Thus smooth muscle myosin filaments might be built from monomers, from dimers, or from higher oligomers. Previous work on smooth muscle myosin has suggested that bipolar dimers, with possibly a 43 nm stagger, may be an important structural theme (Kendrick-Jones and Cohen 1972; Craig and Megerman, 1977; Hinssen et al., 1978; Trybus and Lowey, 1984; Onishi et al.,1984;) For nonmuscle myosin filaments, bipolar or unipolar dimers having a 14-15 nm overlap have been variously proposed as a building unit (Korn and Hammer, 1988; Pasternak et al., 1989; Sinard et al., 1989).

Describing the assembly mechanism in these cases is further complicated by the possibility that the filaments might contain binding sites for several kinds of attacking oligomer, each of different affinity. There is the further possibility of filament breakage, and the related possibility of annealing, of filaments or of small oligomers, either end-to-end or side-by-side. Evidence presented here suggests however that for smooth muscle myosin in physiological buffers these processes are all negligibly slow compared to the rate of monomer exchange at the filament ends. We report rate and equilibrium constants for assembly by this latter route, propose a packing diagram for the filaments, and, based on these data, suggest an outline kinetic model for the assembly pathway.

Results

Molecular packing in the filaments

There are two models in the literature for smooth muscle myosin filaments: that of Craig and Megerman (1977) is a flat sheet of antiparallel myosin dimers, whilst that of Hinssen *et al.* (1978) incorporates a rotation as well as a stagger of neighbouring antiparallel dimers, producing a round filament with heads visible from every aspect. The filaments employed in this study were assembled under similar conditions to those used by Hinssen *et al.*, and under appropriate staining conditions reveal the same axial repeat of layers of crossbridges at ~14 nm (Figure 1). The same preparations viewed under different staining conditions could clearly be seen to have the side polar structure described by Craig, in which heads with opposing polarities emerge from opposite sides of the filament. Symmetrically-related bare ends are obvious, and the other two faces of the filament are devoid of heads (Figure 2). Our data on these *in vitro* self-assembled filaments thus lend support to the view of Craig, based on tilts (Cooke *et al.*, 1989), that smooth muscle myosin filaments are side polar. Notably however, the *in vivo* filaments have a square cross-section, suggesting it is unlikely that they consist of a single sheet of molecules. One possibility, raised originally by Craig (Craig and Megerman, 1977) is that sheets may associate together via their bare faces, to give a filament with a thicker cross section. We infer from the above evidence only that the basic architecture of the filament is that of a side-polar sheet, having a 14 nm axial repeat of crossbridges.

Fraying such filaments in low ionic strength solutions released small oligomers in which it was possible in favourable instances to view directly the overlap between adjacent molecules (Figure 3). The appearances were consistent with a 14 nm parallel overlap between adjacent molecules, suggesting that the previously observed 14 nm repeat in the crossbridge array directly reflects the stagger between adjacent molecules. More surprisingly, we found no evidence for an extensive antiparallel overlap between molecules. Previous work has suggested that an antiparallel 43 nm overlap between molecules is an important structural theme in these filaments. Instead, the appearances suggested an ~14 nm overlap between the tail-tips of antiparallel pairs of molecules (Figure 3). The fraying also permitted a rough head-count. Exact counts were not possible, but the numbers were consistent with the filaments consisting of a single layer of molecules. We cannot exclude however that some molecules were lost in the preparation for electron
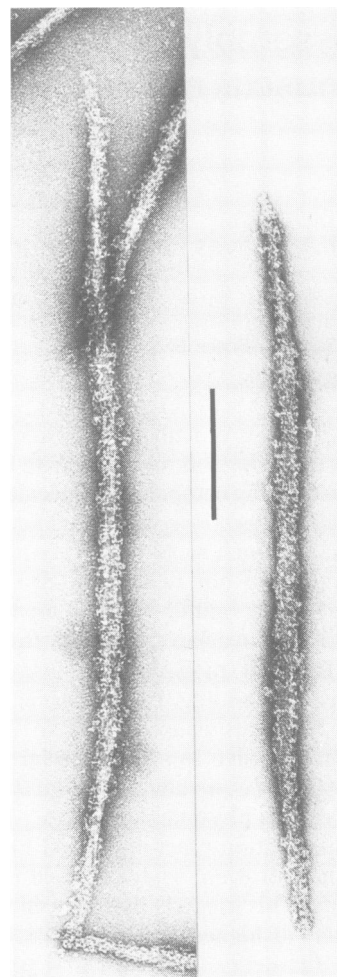

Fig. 1. Uranyl acetate fixed filaments, showing a banding pattern. A sample of the standard filament preparation was mixed with an equal vol of 1% uranyl acetate immediately before application to a carbon-coated 400-mesh copper grid. After a few seconds the grid was rinsed with 6 further drops of 1% uranyl acetate, drained by touching a piece of Whatman no.1 filter paper to its edge and air-dried at room temperature. The periodicity is 14 nm, as determined by comparison with the 40 nm repeat of tropomyosin paracrystals. The scale bar represents 200 nm.

microscopy. Whether the filaments consist of a monolayer sheet, or of 2 or more such sheets, does not affect the kinetic arguments that follow.

Using grids rendered hydrophilic by glow discharge caused the filaments to adhere more tightly to the carbon substrate. The myosin heads in this case were seen to flare away from the filament surface. Knight and Trinick (1984) observed a similar effect following adsorption of skeletal muscle myosin filaments to UV-treated carbon support films. As pointed out by these workers, it is not clear whether this appearance reflects the conformation of the filaments in free solution or not. It is possible that it is an electrostatic effect induced in the vicinity of the highly-charged grids. Whatever its cause, in the present case the flaring conveniently reveals details of the filament organization. In low dose electron micrographs, it was possible to see the molecular packing of individual 2 nm wide myosin tails lying side-by-side across the width of the filament backbone (Figure 4A and B). The backbone was seen to consist of straight, close-packed
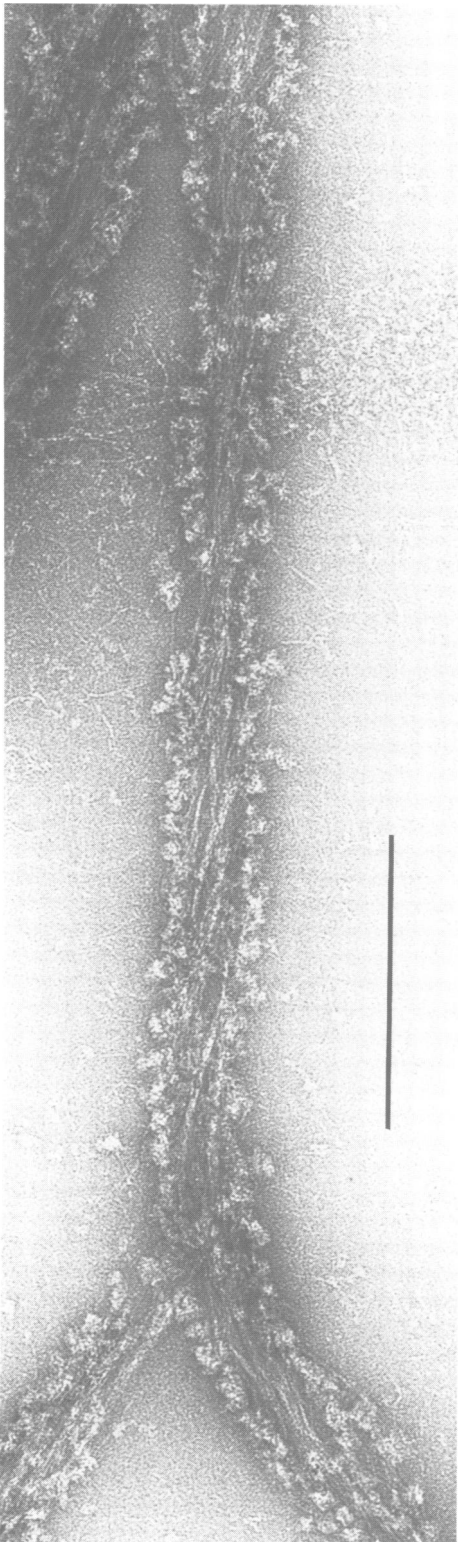
Fig. 2. Myosin filament adsorbed to EM support film, and subsequently negatively stained. A 5 μl drop of the standard filament preparation was applied to 400 mesh Cu grids covered with a freshly-prepared carbon support film. After 5-10 s the grid was partially drained by touching a piece of Whatman no. 1 filter paper to its edge, rinsed with 6 drops of 1% uranyl acetate, drained again and air dried at room temperature. The appearance shown was characteristic of the more deeply-stained regions of the grid. The heads of the myosin molecules emerge with opposite senses from opposite sides of the filament, whilst the top face of the filament is free of such projections. This indicates so-called side-polar packing (Craig and Megerman, 1977). The scale bar represents 200 nm.

molecules. The number of tails across the width of the backbone changed as the myosin tails peeled away from the filament surface, or retracted against it. The observation of straight and close-packed molecules, coupled with the observed 14 nm axial repeat in the array of head-pairs, suggests to us the packing model shown in Figure 5. Each molecule makes a 14 nm overlap with a partner on the opposite side of the filament, and parallel interactions of plus and minus 14 nm with its two same-side neighbours. Within experimental error, this is the same relationship determined independently in the fraying experiments. Taking the M_r of a myosin molecule as 5.30×10^6, the M_r per μm of a monolayer of molecules arranged like this is 7.37×10^7, corresponding to 139 molecules/μm, or 2 molecules/14.4 nm of filament. For comparison, there are 3 molecules/14.4 nm in native skeletal muscle myosin thick filaments. At this stage we cannot judge definitively whether the filaments in our preparation are indeed monolayer sheets, or sandwiches of several such sheets. Published cross-sectional views of side-polar smooth muscle myosin filaments are approximately square, suggesting either that several layers of sheets are indeed present, or that the sheet collapses in solution into a structure having a more compact cross-section. Subsequent calculations in this paper are based on the working assumption that the filament is a monolayer.

Noteworthy features of this monolayer sheet model are (i) the extreme C-terminus of the myosin tail is likely to be critically important for self-assembly—this is consistent with evidence showing that blockage or cleavage of this region abolishes self-assembly (see discussion); (ii) each molecule has an identical packing environment, and therefore presumably an identical affinity for its neighbours, apart from a pair of molecules at each of the filament ends; these pairs overlap with only two, instead of three neighbours, and so are probably more weakly bound to the filament; and (iii) the packing is automatically width limiting, but not length-limiting.

Endwise disassembly

In our standard assembly buffer (essentially a buffered physiological saline), the monomer concentration in equilibrium with filaments in the presence of saturating MgATP is 10 μM, as measured by airfuge ultracentrifugation (Kendrick-Jones et al.,1987). Addition of excess MgATP to filaments below this concentration provokes complete filament disassembly, and allows measurement of a rate constant for disassembly in the near-absence of a competing back-reaction. Using light scattering to report the filament mass concentration, $t_{1/2}$ for diassembly of the filament population is ~30 s (Cross et al., 1986). This value was confirmed for the present series of experiments (data not shown). We observed that this rate was very pH-sensitive. Lowering the pH from 7.3 to 6.7 slowed the rate of disassembly by ~5-fold.

Figure 6 is a montage of micrographs which visualize the disassembly reaction. Aliquots were taken at various times from the reaction, and negatively stained. Disassembly is seen to occur by a progressive shortening of the filaments from their ends. Consistent with this, populations of short filaments were observed in turbidity assays to disassemble faster than populations of long filaments, at constant myosin concentration (data not shown). The more filament ends, the faster the disassembly of the filament population.
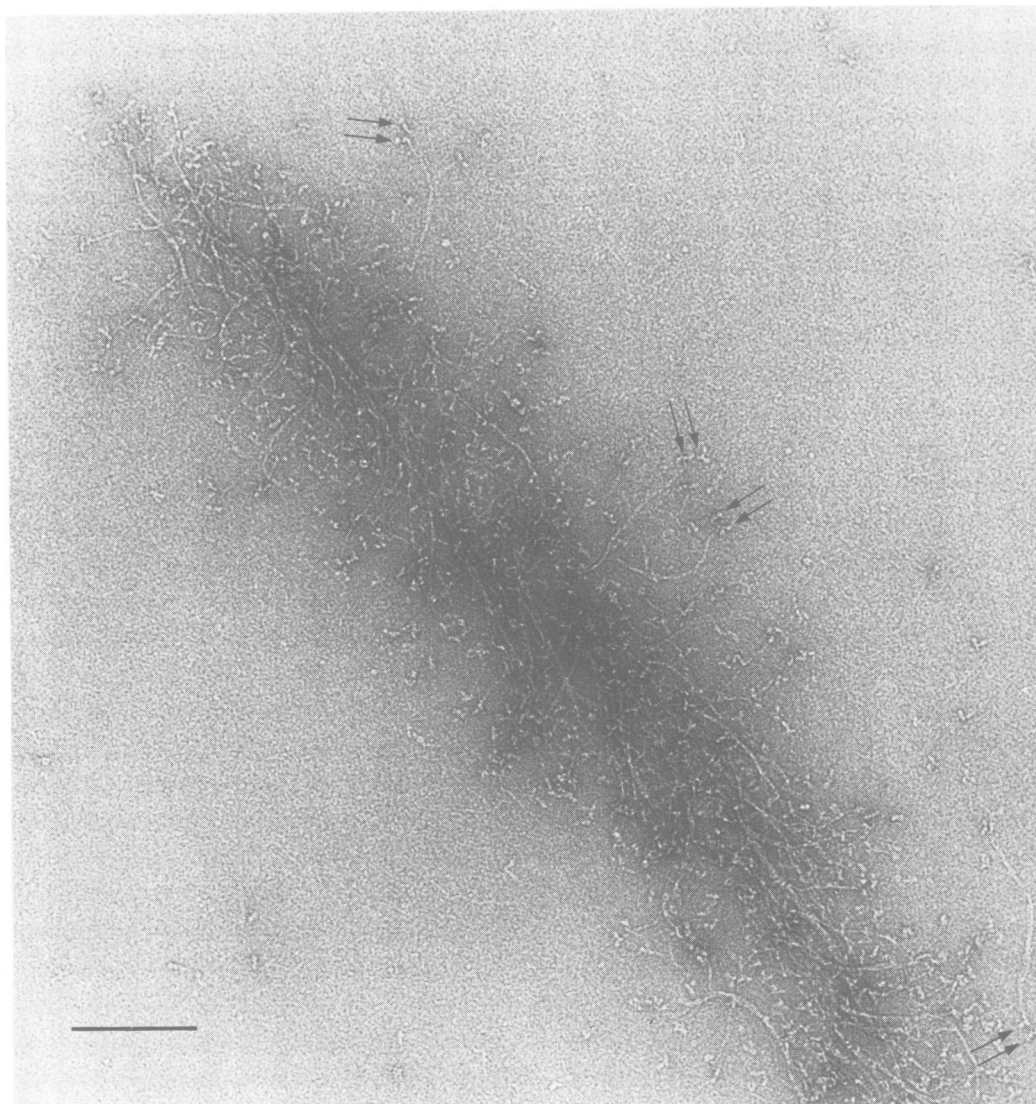
Fig. 3. Fraying of the filaments, induced at low ionic strength. A 5 ml sample of the standard filament preparation was applied to freshly glow-discharged carbon-coated 400 mesh Cu grids. After 5−10 s the grid was rinsed with 6 drops of 5 mM Tris-HCl, 2 mM Na-phosphate, pH 7.0, partially drained by touching the edge of the grid with a piece of Whatman no.1 filter paper, rinsed further with 6 drops of 1% uranyl acetate, drained again and air dried at room temperature. The grids were viewed and photographed under conventional dose conditions in the Philips EM 400 at a nominal magnification of 25 000 ×. The low ionic strength solution has the effect of swelling and fraying the filaments, releasing molecules and small oligomers (arrows) which in favourable instances were well enough displayed to permit the overlap between the molecules to be measured. The scale bar represents 200 nm. The appearances are consistent with a 14 nm parallel and antiparallel staggers between the molecules (see text). Other, larger spacings are occasionally visible. We interpret these as resulting from one or molecules being washed away by the low ionic strength rinse.

Calculated rate constant for dissociation and addition

Using the filament packing model described above, we were able to estimate a microscopic rate constant for the endwise dissociation reaction. The distribution of filament lengths in the preparation is approximately exponential (Cross *et al.*, 1988) and disassembly has an exponential progress curve. A model filament of the mean length of ~ 1 μm contains 139 molecules and disassembles completely by the dissociation of molecules from both ends in 30 s at 20°C, physiological ionic strength and pH 7.3. Each end therefore loses molecules on average at a rate equivalent to 2.1 myosin monomers/s under these conditions.

At steady state, the rate at which molecules condense on to filament ends is equal to the rate at which they dissociate. Taking the free monomer concentration at steady state to be 10 μM in a MgATP-containing buffer, the microscopic rate of association, equal to the rate of dissocation, is

2.1×10^5 M^{-1} s^{-1}. Note that for the purposes of this estimate, the filament model is assumed to be a monolayer of molecules, and that the further assumption is made that the exchanging species (the building block) is a myosin monomer. This assumption is justified in the following section.

Pressure jump experiments: the building unit

Under the assembly conditions used in this paper, the assembly equilibria were pressure sensitive (in the same buffer but with pH adjusted to 7.0 or below, they were not). The degree of disassembly was proportional to the amount of pressure applied. Rapid release of this excess pressure permitted reassembly. The rate constant of the recovery provides a measure of the rate constant for subunit addition, whilst the dependence of the observed rate on excess monomer concentration (equivalent to excess pressure, since
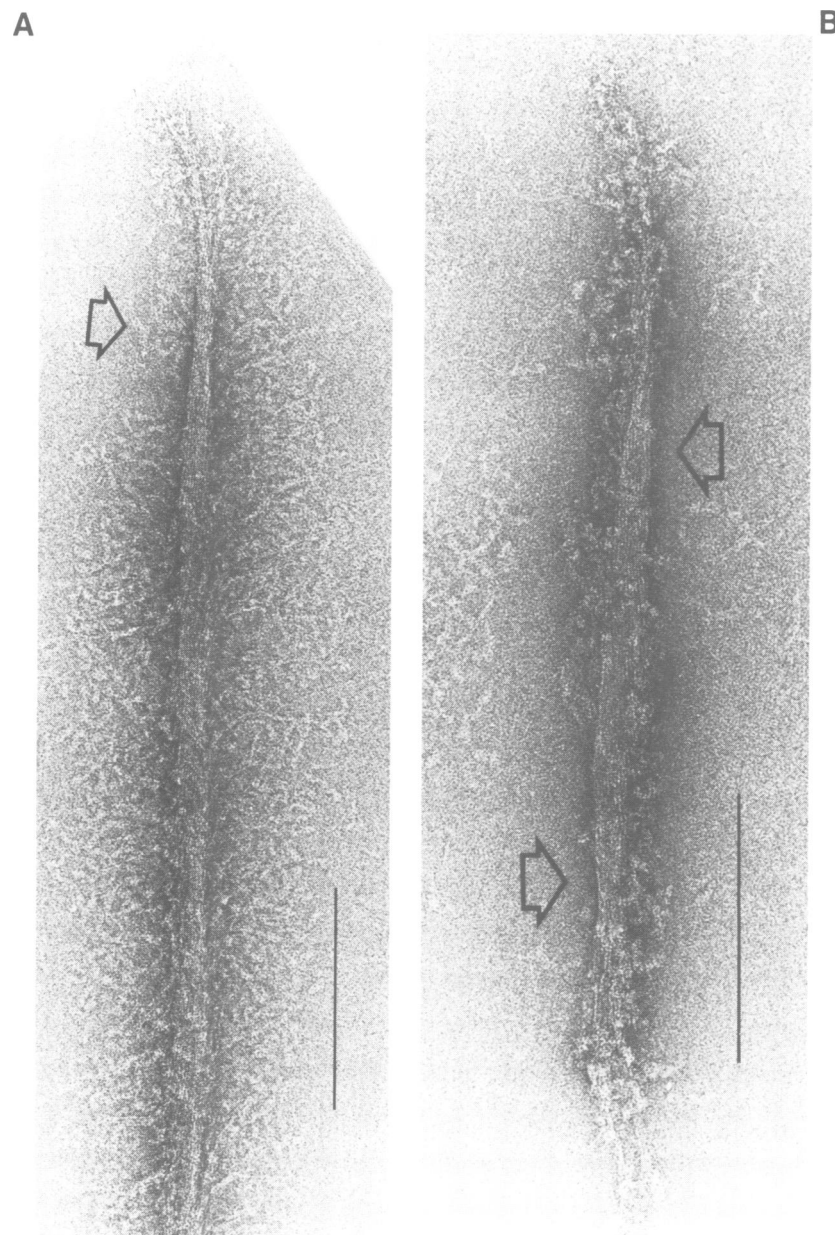
Fig. 4. Fine structure of the tips of two *in vitro* self-assembled myosin filaments. A 2 μl drop of the standard filament preparation was applied to freshly glow-discharged carbon-coated 400 mesh Cu grids. After 5 s, the grid was drained by touching a piece of Whatman no.1 to its edge, then rinsed with 6 drops of 1% uranyl acetate, drained again and dried in air at room temperature. The grids were photographed at a nominal magnification of 43 000 under low dose conditions in a Philips CM12 electron microscope with a LaB$_6$ filament operated at 80 kV. The electron dose was 20 e Å^{-2}. We found that higher doses tended to degrade the fine detail of the backbone structure. The scale bars represent 200 nm. (A) In this type of image the myosin heads are seen as a diffuse cloud of material, extending a considerable distance from the surface of the filament. The side-polar appearance is still clear, most notably as the bare-edge at the filament tip (arrow). In the shorter filament shown in (B), the heads are tighter against the filament backbone and the backbone is thickened by the annealing of a longer length of each myosin tail to the backbone. Two symmetry-related bare edges are apparent (arrows). In both cases, fine longitudinal striations, running at a shallow angle to the long axis of the filament, are visible in the filament backbone. We think these are the tails of single myosin molecules, because they have the same dimensions as single myosin molecules which can occasionally be seen in the background (not shown). The striations are strikingly straight and may be followed in some cases for distances greater than the length of a myosin molecule. The appearances suggest that the molecules are straight and close packed within the filament backbone.

the two are linearly related) indicates the reaction order. Thus Davis (review, 1988) observed for striated muscle myosin filaments at pH 8.0 that the observed rate of reassembly was dependent on the square of the free monomer concentration, consistent with a dimerization being rate-limiting in the reassembly. In the present case, the degree of pressure-induced filament disassembly (as judged by the amplitude of the change in the transmission signal) was also proportional to the applied pressure, but the major phase of the recovery from pressure-induced disassembly appeared to be first order, since it was well fitted by a single exponential. Each trace also had a minor initial component whose amplitude was pressure-independent, and whose rate was too fast to resolve. We speculate that this reflects a conformational change in the heads array. That the major phase in each case was first order indicates that the initial
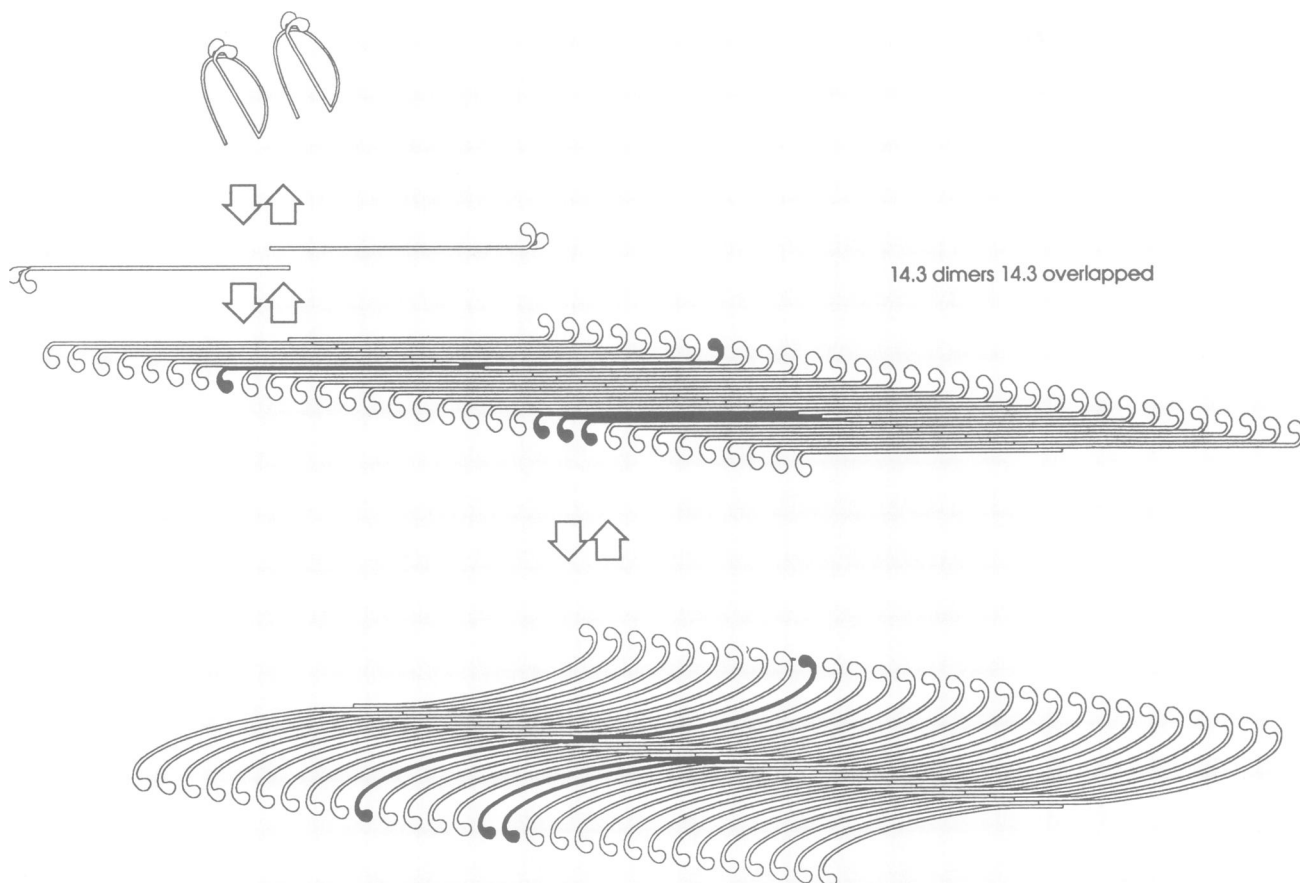
14.3 dimers 14.3 overlapped

Fig. 5. Scale diagram of filament packing. For clarity, only one head of each molecule is shown. The molecules all have an identical packing environment, apart from the molecules at the ends of the filament. The molecules in the interior of the filament are shown straight and close packed into a sheet. Each is postulated to overlap two parallel partners by ± 14 nm, and one antiparallel partner by 14 nm. The filament is shown equilibrating between tight and flared conformations, corresponding respectively to the structures shown in Figure 4B and A.

rate of reassembly was linearly dependent on monomer concentration over the range of pressures accessible to us (Figure 7), suggesting that monomers, rather than dimers, add to filaments. Microscopic reversibility would then suggest that the dissociating species is the same as the associating species, in other words that monomers are also the dissociating species.

Endwise assembly onto existing gizzard myosin filaments

Titrating a population of short smooth muscle myosin filaments with incremental amounts of MgATP induces incremental amounts of disassembly of filaments into 10S monomers (Cross *et al.*, 1986). The monomers which are released from the filaments adopt the looped (10S) conformation and consequently hydrolyse their MgATP very slowly, at 2×10^{-4} s^{-1} at 20°C. Reassembly is rate-limited by this reaction. If substoichiometric ATP is added to a population of filaments (Figure 8A), the filaments shorten, but the number of filaments remains the same. Reassembling molecules appear to join the ends of these existing filaments, because the population eventually recovers its original numbers and length distribution (Figure 8B). Addition of saturating MgATP to the same starting population yields a radically different result. In this case, disassembly of the starting population is complete, there are no filaments present to act as seeds for reassembly, and new filaments must be initiated. Recovery then leads to the formation of much longer filaments (Figure 8C), suggesting that as soon as

relatively few nuclei are formed, reassembling molecules preferentially add to their ends, rather than forming themselves into more nuclei. The result is thus consistent with a mechanism in which nucleation is kinetically more awkward than propagation, meaning that myosin molecules preferentially react with the end of an existing filament, rather than with one another to initiate (nucleate) a new filament.

Spontaneous shearing and annealing are negligibly slow

Actin and tubulin polymers at steady state tend to get longer, and fewer, because the polymers tend to join together end-to-end (anneal). We tested for annealing of myosin filaments by deliberately shortening the filaments by mechanical shearing, and looking for a recovery of length. Preparations of filaments shortened in this way retained their new length distributions for tens of hours (Figure 9), indicating that annealing is negligibly slow under the conditions assayed. This suggests that spontaneous shearing of myosin filaments is also rare.

Discussion

A key role of the C-terminus of myosin in filament self-assembly

A short, C-terminal region of the tail of myosins II from many sources has been shown to be an essential requirement for self assembly, both of myosin and of myosin rod (Korn
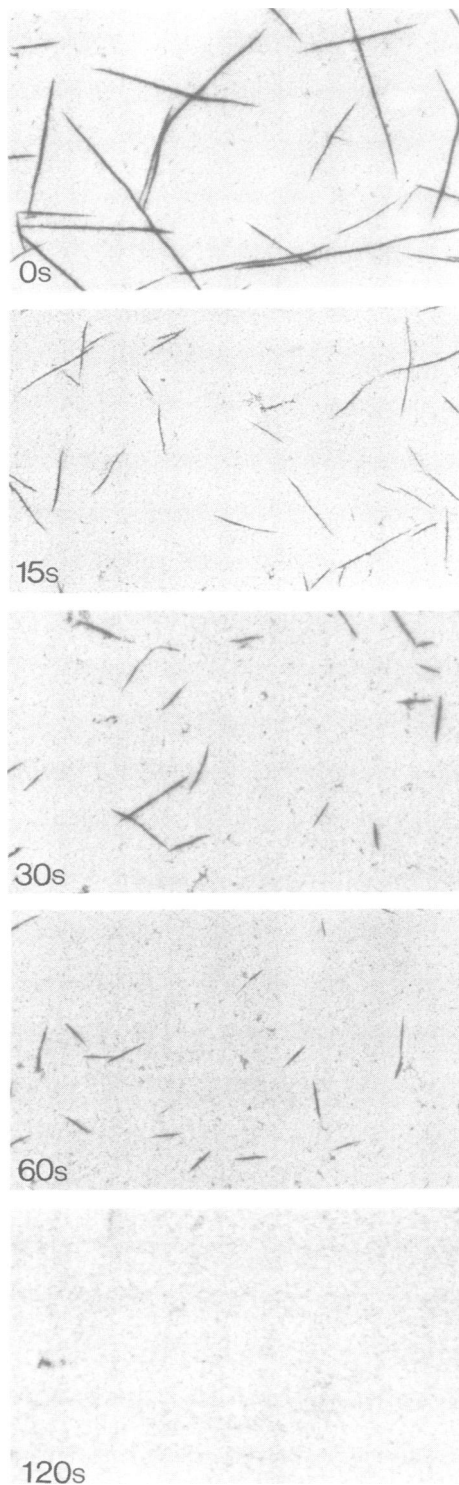
Fig. 6. Endwise disassembly of filaments, visualized by negative stain microscopy. Disassembly of a sample of the standard preparation of filaments (uppermost frame) was initiated by addition of a 2-fold molar excess of MgATP over myosin heads. Samples were withdrawn from the reaction mixture at the intervals shown and applied to freshly glow-discharged carbon grids. After 2−3 s the grid was rinsed with 1% uranyl acetate, drained by briefly touching a piece of Whatman no. 1. filter paper to its edge and set to dry, and the next sample taken. Conventional dose micrographs were recorded at a nominal magnification of 2500×, which allowed entire grid squares to be observed. The areas shown were judged by eye to be representative of the populations. The reported half time for disassembly, 30 s (Cross *et al.*, 1986) was confirmed for the present series of experiments by turbidimetry (data not shown).

and Hammer, 1988). It has hitherto been unclear what the role of this section of the myosin tail might be. For smooth muscle myosin, it was shown that progressive proteolytic truncation of this region produced a progressive change in solubility (Cross and Vandeckerckhove, 1986). The same thing has recently been shown to be true for brush border myosin II using site-directed mutagenesis (Cross *et al.*, 1991). The packing diagram proposed here provides a rationale for the importance of this region, by suggesting that it is critical for the formation of symmetrical tail-tip to tail-tip antiparallel dimers. Two things follow, first, the observed parallel 14 nm interactions between molecules are weak, relative to the antiparallel interactions. This is consistent with the observation (Figure 3) that considerable flaring of the head-ends of molecules away from the filament backbone is possible, without snapping the filament. Second, the formation of antiparallel dimers is an absolute requirement for nucleation and elongation. This is consistent with the efficient blocking of self-assembly of myosin by antibodies to the tail-tip (e.g. Citi *et al.*, 1989), but is at first site at odds with our proposal that monomers rather than dimers are the exchanging unit (the building unit) for filaments. The difficulty is removed by supposing that dimers form at the filament ends, rather than in free solution. Dimerization at the filament ends would, we believe, be favoured over dimerization in free solution, because one of the reactants is immobilized. The filament end in this case acts something like a catalyst. A consequence of this mechanism is that the structure of the filament end would oscillate between two states, that in which an unpaired monomer is bound, and that in which a completed dimer is bound. There would be a corresponding oscillation in the affinity of the filament end for incoming monomers.

Kinetics of nucleation and propagation

It was shown above (Figure 7) that supplying nuclei (in the form of short myosin filaments) to the assembly reaction resulted in molecules preferentially joining onto the ends of the nucleii, rather than initiating fresh filaments. Accordingly it seems clear that addition of molecules to the ends of existing filaments is kinetically more favourable than fresh nucleation. Nonetheless it is straightforward in practice to favour the nucleation reaction over the addition (elongation) reaction, for example by diluting a high concentration of myosin in solution in high salt into low salt. By contrast, long filaments may be formed by supplying molecules slowly to the assembly reaction (Sobieszek, 1972). As we have shown above, two entirely different stable length distributions of filaments may be generated under precisely the same solvent conditions by supplying molecules to the assembly reaction at different rates. We found that an adequate model of the assembly process can be built by assuming, as argued above, that the relative difficulty of filament initiation (nucleation) is due to the necessity to form dimers in solution, whereas growth (elongation) requires only monomers. In this case, the rate of nucleation will vary as the square of the monomer concentration, whilst the rate of propagation will vary linearly with the monomer concentration. Elongation is favoured over nucleation at low monomer concentrations, but nucleation becomes progressively more favourable as the monomer concentration is increased. The nucleation of new filaments thus requires that monomers be supplied to the assembly reaction faster than they are consumed by the elongation reaction.
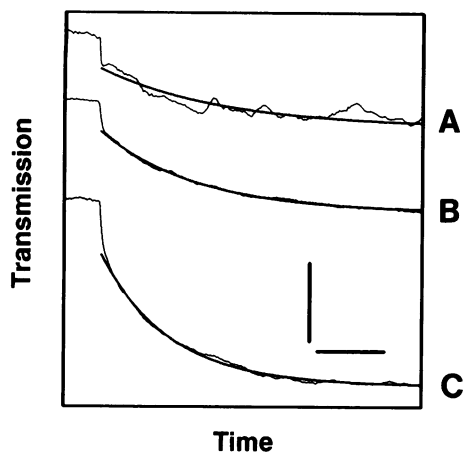
753

Time

Fig. 7. Pressure jump experiments. The experiments were done under the standard conditions for filament assembly, except that the pH was increased from 7.3 to 7.5. In the experiment shown, the myosin concentration was 1 mg ml^{-1}.Each trace represents the observed relaxations at different pressures on the same sample, and the best fit single exponential is superimposed. The percentage change in turbidity is referenced to the stable signal at 1 atmosphere, and the vertical scale bar represents 1% of the signal change. The horizontal scale bar represents 1 s for (A) and (B), and 2 s for (C). (A) average of 3 successive relaxations from 50 atm. applied pressure. $k = 0.61$ s^{-1}, amplitude -0.61%. (B) average of 5 successive relaxations from 100 atm. applied pressure. $k = 0.71$ s^{-1}, amplitude -0.91%. (C) average of 5 successive relaxations from 150 atm. applied pressure. $k = 0.52$ s^{-1}, amplitude $= 1.5\%$.

The overall behaviour of this type of model is represented in Figure 10B. The solid line in this figure corresponds to classical critical concentration behaviour (Oosawa and Asakura, 1975), in which a constant monomer concentration exists in equilibrium with a variable polymer concentration. The dashed line corresponds to a zone of supersaturation which is predicted by the model under discussion. As the monomer concentration is slowly increased from a low value, the monomer solution reaches a concentration which will support elongation, but not nucleation. A further increase in monomer concentration allows nucleation to occur. Elongation of the nuclei is then rapid, and the monomer concentration decays back to its critical value (see also legend to Figure 10).

Predicted consequences for the cell

It is difficult, based on the present observations, to make firm predictions about myosin assembly *in vivo*, because clearly the native filaments are assembled in the presence of other proteins, primarily actin, which may influence the assembly process. We believe nonetheless that the principal finding described here, that a nucleation—elongation mechanism applies, is likely to hold true in the cell. Such a mechanism provides intriguing possibilities for the regulation of filament geometry. Thus the preference of incoming monomers for the ends of existing filaments means that fresh nuclei will form only if monomers are made available for assembly faster than they are consumed by the elongation reaction. We predict therefore that the rate at which molecules exit from the 10S storage state (and thus become available for assembly) will affect the number and length of filaments formed. This step can be regulated *in vitro* by phosphorylation of the regulatory light chain, and the obvious possibility is that its regulation *in vivo* would
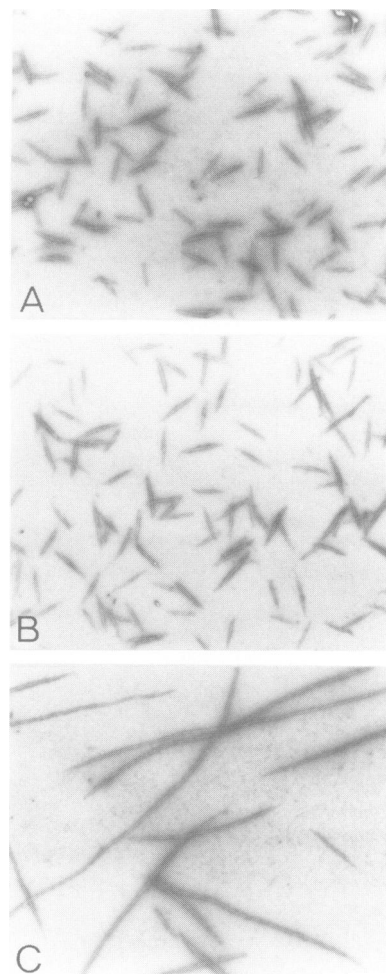

Fig. 8. Preexisting filaments as templates for assembly. Different amounts of MgATP were added to aliquots of the filament preparation shown in (A), causing various degrees of disassembly (not shown). As the MgATP was hydrolysed, reassembly occurred (Cross *et al.*, 1986). The final length distribution of the filaments varied according to how much MgATP was added. For substoichiometric MgATP, disassembly was limited, and reassembly occurred on to the ends of existing filaments, producing a regrowth of the original population (B). For superstoichiometric MgATP, disassembly was complete, and reassembly required fresh nuclei to be formed. Evidently, rather few nuclei are formed, and much growth occurs, producing the population of long filaments shown in (C). There was no obvious drift of the length distribution in either case after a further 2 h (not shown).

control filament length and number, as well as the position of the assembly—disassembly equilibrium. That assembly occurs by exchange of molecules at the filament ends suggests secondly the possibility of stabilizing an entire filament by modification of its ends. It will be interesting, for example, to see whether a cap of phosphorylated myosin acts to stabilize a filament of unphosphorylated myosin.

Conclusions

In vitro-assembled smooth muscle myosin filaments were found to be side polar sheets, in which adjacent molecules overlapped by ~ 14 nm. They were found to assemble and disassemble by molecular exchange at their ends, at limiting rates correponding to ~ 2 monomers per second per filament end. A range of monomer concentration was shown to exist in which elongation of existing filaments can occur, but nucleation of fresh filaments cannot. This tendency for
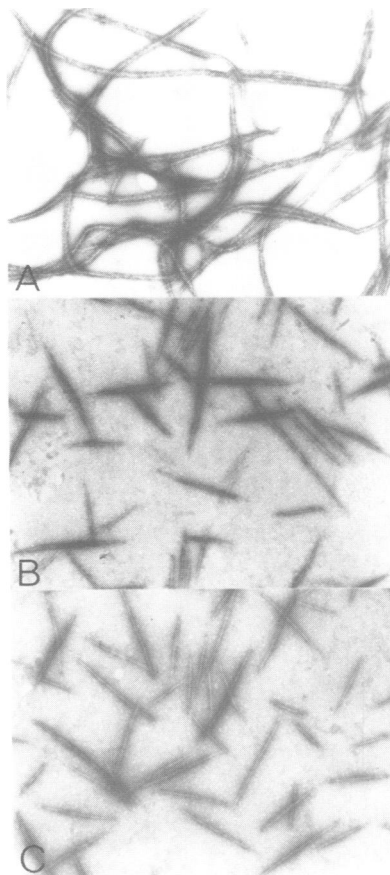
Fig. 9. Shearing experiment. The standard preparation of filaments (A) was sheared by 5 passes through a 27 gauge syringe needle. This treatment broke the long filaments into shorter filaments (B). The preparation retained its new, shorter length distribution even after incubation overnight at 4°C (C), suggesting that little or no end-to-end reannealing of the filaments had occurred over this incubation period. The critical concentration of monomers in equilibrium with polymer was unchanged by the shearing, as determined by airfuge ultracentrifugation (data not shown).

myosin molecules to condense on to the ends of existing filaments is the dominant property of the self-assembly. Consequently if new filaments are to nucleate in the presence of existing filaments, molecules must be added to the assembly reaction faster than they can add to existing filament ends.

Materials and methods

Preparation of myosin and myosin filaments

Myosin was prepared from glycerinated gizzard muscle, exactly as described by Kendrick-Jones et al., (1983). The myosin was stored in 4× assembly buffer supplemented with 50% glycerol, at a concentration of 10-20 mg ml^{-1}. Short filaments were assembled by the rapid addition of 3 vol of water, followed by dilution in 1× assembly buffer to give a final myosin concentration in the region of 0.5 mg ml^{-1}. These filaments were then disassembled by the addition of slightly superstoichiometric MgATP, the solution clarified by airfuge ultracentrifugation, and the supernatant incubated overnight on ice. Assembly buffer is 150 mM NaCl, 10 mM imidazole, 1 mM MgCl$_2$, 0.5 mM DTT, 0.5 mM EGTA, pH 7.3 at 20°C.

Spectrophotometry

Myosin concentration was estimated spectrophotometrically using an A$_{280\ nm}$ in 1 cm cells of 0.45 mg^{-1} ml^{-1}. Filament concentrations were followed by measuring the apparent absorption at 340 nm in a temperature controlled spectrophotometer. Data were collected on chart paper, and digitized where necessary for analysis using a graphics tablet. Turbidity was linearly related to polymer concentration as determined in a dilution
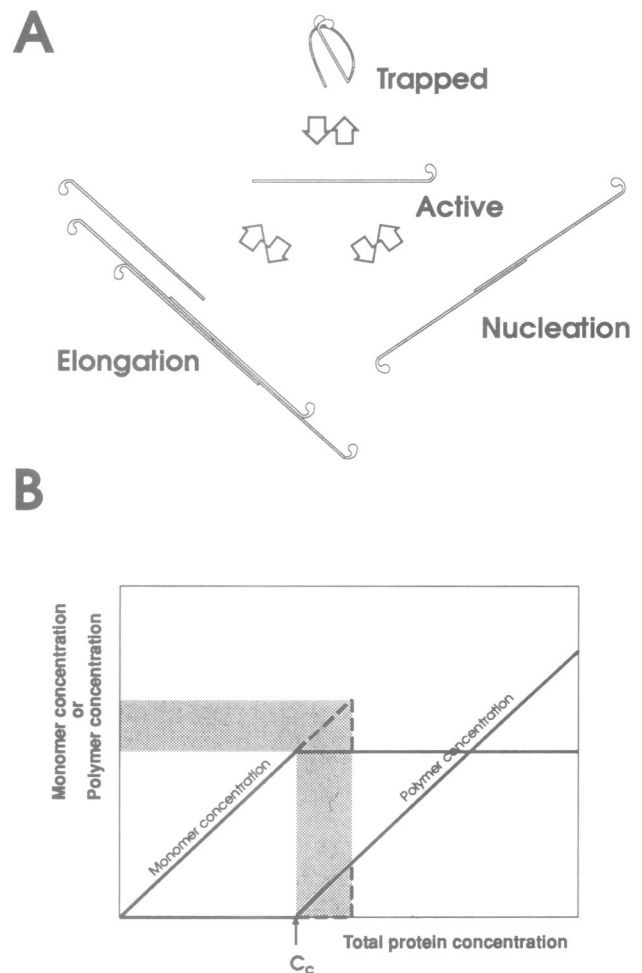

Fig. 10. Behaviour of a model mechanism for filament self-assembly. The model postulates (A) a relatively simple branched pathway, in which the nucleation and elongation reactions compete for monomers. Nucleation requires at least the reaction of two monomers, whereas elongation involves the binding of one monomer at a time to the filament end. The rate of nucleation therefore varies as the square of the monomer concentration, whilst the rate of elongation varies directly with monomer concentration. (B) illustrates one consequence of such a mechanism, which is that the system can exhibit supersaturation behaviour. A supersaturated monomer solution (shaded area) arises when the monomer concentration is sufficient for the elongation reaction to proceed, but insufficient for nucleation. The dotted routes in the diagram represent the pathways leading to a supersaturated monomer solution. These are only followed when the monomer concentration is slowly increased from a very low value. When the monomer concentration reaches that required for nucleation, an explosive polymerization is predicted to occur, with the monomer concentration decaying rapidly to its steady-state value (the critical concentration, C$_c$).

series, and as predicted for disperse polymers of uniform width and of length greater than ~3.5 times the wavelength of the illuminating light (Berne, 1974).

Electron microscopy

Negative staining was done on carbon films using 1% uranyl acetate. The films were prepared by evaporation of carbon rods on to freshly cleaved mica at 10^{-5} atmospheres in an Edwards machine, and picked up right sides up on 400 mesh copper grids. Glow discharge of these grids was performed at a nominal 10^{-3} atmospheres pressure in air, and the grids were used within 30 min.

Pressure jump methods

The pressure relaxation equipment was that described by Davis and Gutfreund (1976). Transmission was observed at 370 nm using a tungsten light source and a Farrand monochromator. Samples were exposed to elevated pressure

and allowed to equilibrate for a few seconds before the pressure was released back to ambient pressure. The rapid release mechanism of Davis and Gutfreund was used which had a release time of 200 μs.

The data were collected as 1024 eight bit data points on a datalab DL 905 transient recorder and transferred to a Hewlett Packard 310 computer for analysis using a nonlinear least squares fitting routine.

Acknowledgements

References

Berne,B.J. (1974) *J. Mol. Biol.*, **89**, 755.

Castellani,L., Elliott,B.W., Jr. and Cohen,C. (1988) *J. Musc. Res. Cell Motil.*, **9**, 533–540.

Citi,S. and Kendrick-Jones,J.(1988) *J. Mol. Biol.*, **188**, 369–382.

Citi,S., Cross,R.A., Bagshaw,C.R. and Kendrick-Jones,J. (1989) *J. Cell Biol.*, **109**, 549–556 .

Cooke,P.H., Fay,F.S. and Craig,R. (1989) *J. Musc. Res. Cell Motil.*, **10**, 206–220.

Craig,R. and Megerman,J. (1977) *J. Cell Biol.*, **75**, 990–996.

Cross,R.A. (1988) *J. Musc. Res. Cell Motil.*, **9**, 108–110.

Cross,R.A. Cross,K.E. and Sobieszek,A. (1986) *EMBO J.*, **5**, 2637–2641.

Cross,R.A. and Vanderkerckhove,J. (1986) *FEBS Lett.*, **200**, 355–360.

Cross,R.A., Citi,S. and Kendrick-Jones,J. (1988) *Biochem. Soc. Trans.*, **16**, 501–503.

Cross,R.A., Hodge,T.P. and Kendrick-Jones,J. (1991) *J. Cell Sci.*, in press.

Davis,J.S. (1981) *Biochem. J.*, **197**, 301–308.

Davis,J.S. (1985) *Biochemistry*, **24**, 5263–5269.

Davis,J.S. (1988) *Annu. Rev. Biophys. Biophys. Chem.*, **17**, 217–239.

Davis,J.S. and Gutfreund,H. (1976) *FEBS Lett.*, **72**, 199–207.

Davis,J.S., Buck,J. and Greene,E.P. (1982) *FEBS Lett.*, **140**, 293–297.

Hinssen,H., DiHaese,J Small,J.V. and Sobieszek,A. (1978) *J. Ultrastruc. Res.*, **64**, 282–302.

Josephs,R. and Harrington,W.F. (1966) *Biochemistry*, **5**, 3474–3487.

Josephs,R. and Harrington,W.F. (1968) *Biochemistry*, **7**, 2834–2847.

Kendrick-Jones,J., Szent-Gyorgyi,A.G. and Cohen,C. (1971) *J. Mol. Biol.*, **59**, 527–529.

Kendrick-Jones,J., Cande,W.Z.,Tooth,P.J., Smith,R.C. and Scholey,J.M. (1983) *J. Mol. Biol.*, **165**, 139–162.

Kendrick-Jones,J., Smith,R.C., Craig,R. and Citi,S. (1987) *J. Mol. Biol.*, **198**, 241–252.

Knight,P.J. and Trinick,J.. (1984) *J. Mol. Biol.*, **177**, 461–482 .

Korn,E.D. and Hammer,J.A.III (1988) *Annu. Rev. Biophys. Biophys. Chem.*, **17**, 23–45 .

Megerman,J., and Lowey,S. (1981) *Biochemistry*, **20**, 2099–2110.

Niederman,R. and Peters,L.K. (1982) *J. Mol. Biol.*, **161**, 505–517.

Onishi,H. and Wakabayashi,T. (1984) *J. Biochem.*, **95**, 903–905.

Oosawa,F. and Asakura,S. (1975) *Polymerisation of Proteins*. Academic Press, London.

Pasternak,C., Flicker,P.F., Ravid,S. and Spudich,J.A. (1989) *J. Cell Biol.*, **109**, 203–210.

Pollard,T.D. (1982) *J. Cell Biol.*, **95**, 816–825.

Reisler,E., Smith,C. and Seegan,G. (1980) *J. Mol. Biol.*, **143**, 129–145.

Sobieszek,A.(1972) *J. Mol. Biol.*, **70**, 741–744.

Sinard,J.H., Stafford,W.F. and Pollard,T. (1989) *J. Cell Biol.*, **109**, 1537–1547.

Small,J.V. (1988) *Nature*, **331**, 568–569.

Spudich,J.A. (1990) *Cell Regulation*, **1**, 1–11 .

Trybus,K.M. and Lowey,S. (1987) *J. Cell Biol.*, **105**, 3021–3030.

Trybus,K.M. and Lowey,S. (1987) *J. Cell Biol.*, **105**, 3021–3030.

Trybus,K.M. and Lowey,S. (1984) *J. Biol. Chem.*, **259**, 8564–8571.

Yumura,S. and Fukui,Y. (1985) *Nature*, **314**, 195–196.